

# DESIGN CONSIDERATIONS OF TRANSMISSION LINE SUPERCONDUCTORS FOR FAST-CYCLING ACCELERATOR MAGNETS\*

H. Piekarz\*\*, FNAL, Batavia, IL 60510, U.S.A

## Abstract

Novel design options of HTS and LTS superconductor lines for fast-cycling accelerator magnets are presented. The cryogenic power losses in using these conductors in transmission line application to energize the accelerator magnet string are discussed. A test arrangement to measure power loss of the proposed superconductor lines operating up to 2 T/s ramp rate and 0.5 Hz repetition cycle is described.

## MOTIVATION

There are a number of large scale fast-cycling proton synchrotrons considered for a possible construction in a near future, e.g. PS2 at CERN [1] and DSFMR [2] at Fermilab. The use of the superconducting magnets rather than the conventional ones allows one to significantly reduce magnetic core sizes and consequently to save valuable space in the accelerator tunnel. This is especially true for the DSFMR with its two accelerator rings to be fit in the existing Tevatron tunnel. Powering the magnet string with a transmission-line conductor allows further minimization of the space required for the magnets, and in addition the magnet interconnections are also much simplified providing convenient space for the corrector magnets. Although there have been already considerable efforts [3] aimed at designing fast-cycling superconducting magnets new approaches are needed to reduce the dynamic power losses to a level that is acceptable for a large synchrotron. With this in mind we are considering a novel arrangement of both the HTS single-filament tape strands and the LTS wire strands to construct the superconducting power lines for the fast-cycling magnets.

## HTS AND LTS SUPERCONDUCTOR LINE DESIGN CONSIDERATIONS

A brief description of the HTS and the LTS conductor conceptual design is given in [4]. These conductors can be arranged as the power lines which are wrapped around the magnetic core in a conventional magnetic design, or used as the straight-through power lines in a transmission-line mode of energizing the magnet. The size of the individual line has been chosen to minimize the space required for

\* This work has been authored by Fermi Research Alliance, ILC under DOE Contract DE-AC02-07CHI1359

\*\* On behalf of Fast-Cycling Superconducting Magnet Group at FNAL: J. Blowers, D. Harding, S. Hays, Y. Huang, A. Klebaner, T. Peterson, H. Piekarz, V. Shiltsev, J. Theilacker and D. Wolff

the line within a magnetic core, and also to facilitate bending of the line at rather small radius as it may be required for the magnet interconnections. A conceptual design of both the HTS and the LTS conductor lines is shown in Fig. 1. Both these lines were designed to carry about the same transport current of  $\sim 20$  kA. The HTS line

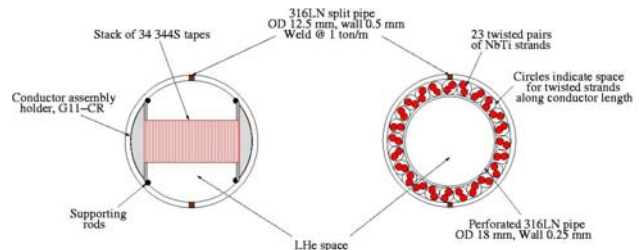


Fig. 1 Conceptual designs of HTS and LTS conductors

consists of 34 the 344S YBCO tapes of the American Superconductor Inc., while the LTS line consists of 46 NbTi strands of the SSC outer dipole type. The major difference between the two approaches is the allowable temperature margin ( $\sim 20$  K for the HTS and  $\sim 2$  K for the LTS) for the superconducting state above the normal operating temperature of 4.5 K. We will evaluate below supercritical helium flow pressure drop and the allowable heat transfer from the flowing helium to conductor strands in these lines as a function of the LHe flow rate (which is equivalent to the Reynold's Number).

The cryogenic parameters of proposed CICC (Cable-In-Conduit-Conductor) HTS and LTS conductor lines are listed in Table 1. We assume use of supercritical helium

Table 1: Cryogenic parameters of proposed conductors

CICC geometry	HTS	LTS
Pipe outer diameter [mm]	12.5	12.5
Pipe inner diameter [mm]	11.5	11.5
Number of strands	35	46
Single strand area [mm <sup>2</sup> ]	0.90	0.43
Total strand area [mm <sup>2</sup> ]	31.5	19.8
Void fraction	0.70	0.81
LHe flow area [mm <sup>2</sup> ]	73	84
Pipe perimeter [mm]	36	64
Total strand perimeter [mm]	263	120
Cooled perimeter [mm]	300	184
Hydraulic diameter [mm]	0.97	1.83

of average temperature 4.75 K and 0.26 MPa pressure, with only minimal rise of temperature (e.g.  $< 0.2$  K) and

minimal pressure drop (e.g. < 0.05 MPa) allowed while the liquid is passing through conductor line. This allows one to keep the basic physical parameters (density, specific heat, viscosity) of the flowing liquid He within rather a narrow range which helps make predictions of a friction factor more reliable.

The pressure drop  $\Delta P$  in a pipe is directly proportional to the friction factor  $F_f$  as indicated in formula (1) from [5]:

$$\Delta P/L = 0.5 F_f [P_{\text{cooled}} \times (dm/dt)^2] / [\rho \times (A_{\text{flow}})^3] \quad (1)$$

where  $L$  is the pipe length,  $P_{\text{cooled}}$  is the cooled perimeter,  $dm/dt$  is the flow rate,  $\rho$  is the LHe density and  $A_{\text{flow}}$  is the helium flow cross-section area. For a turbulent flow in a smooth pipe the friction factor,  $F_f$  is calculated using an empirical formula (2):

$$F_f = 0.3164 Re^{-0.25} \quad (2)$$

where Reynolds Number  $Re = 4 [(dm/dt)/(k \times P_{\text{cooled}})]$  and  $k$  is the viscosity of the fluid. For a non-smooth pipe a “roughness” parameter  $\epsilon/D$  [6], with  $\epsilon$  being a size of a continuing disturbance and  $D$  diameter of the pipe, is used to modify the friction factor projected with formula (2). Based on the graphs given in [6] we scale the  $F_f$  parameter for Reynolds Numbers of (2600 – 26000), corresponding to the LHe (4.7 K @ 0.26 MPa) flow rates of (0.5 – 5) g/s in the proposed LTS and HTS conductor lines. The result is shown in figure 2. We observe that the friction factor is

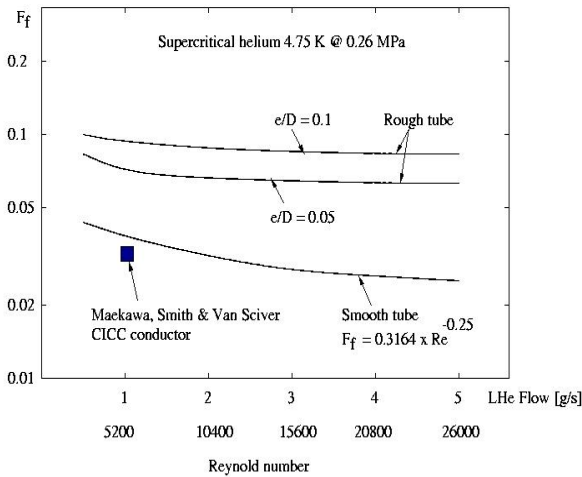


Fig.2 Friction factor in rough tubes of  $\epsilon/D = 0.05$  and  $0.1$  as compared to that of a smooth tube

higher at the lower flow rates, and it increases further (not shown in the figure) in the laminar flow region which is below the  $Re \sim 2600$ . A more detailed dependence of the friction factor on the roughness parameter,  $\epsilon/D$ , is shown in figure 3 for the Reynolds Numbers of 4000, 10000 and 20000. It is interesting to note that in the experiment [5]

with a large number of strands in the CICC conductor the friction factor was found consistent with a smooth tube. This may suggest that if the strands have smooth surface their presence in the cable-in-conduit pipe does not necessarily increase friction factor for the helium flow. Consequently for the HTS conductor with 344S tapes of a very smooth surface we assumed the friction factor  $F_f \sim 0.035$ , or consistent with a smooth tube. For the LTS conductor with the twisted pairs of the NbTi strands, however, we assumed that the wire diameter constitutes “roughness”, and so the friction factor  $F_f$  would be  $\sim 0.1$  in this case.

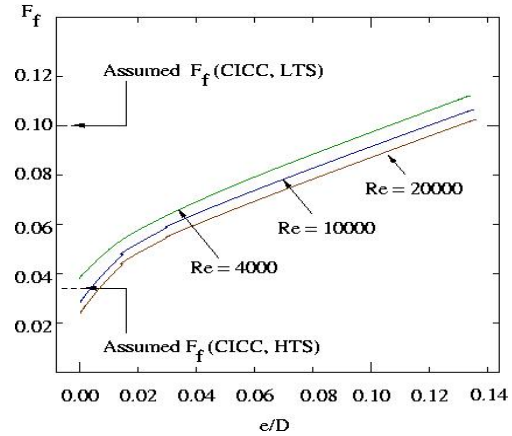


Fig. 3 Friction factor as a function of roughness for the Reynolds Numbers of 4000, 10000 and 20000

With the friction factors determined in this way we can estimate pressure drop for the liquid helium flow in both LTS and HTS conductors using the formula (1). The results for the supercritical helium (4.7 K @ 0.26 MPa) are shown in figure 4. One can see that the pressure drop increases strongly with increase of the helium flow rate, and the pressure drop is higher for the HTS conductor.

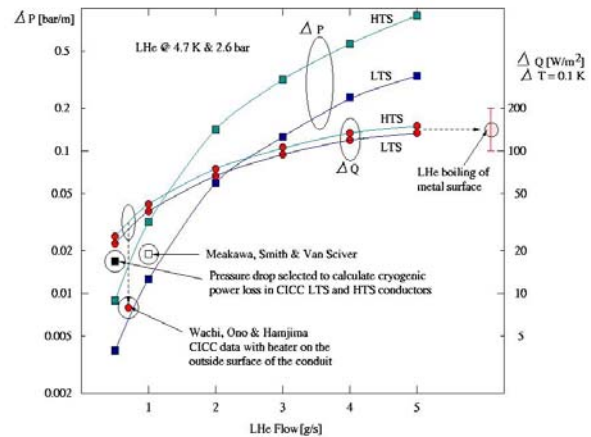


Fig. 4 Pressure drop in LTS and HTS conductors and ideal heat transfer

The available heat transfer from the flowing liquid helium to the conductor strands inside the CICC tube is a second most important factor in the conductor design. The ideal steady-state turbulent flow heat transfer  $Q$  in a smooth pipe is given in [7] as:

$$Q = 0.0259 (k/D_h) \times \text{Re}^{0.80} \times \text{Pr}^{0.4} \times (T_c / T_{\text{He}})^{-0.716} \quad (3)$$

where  $D_h$  is hydraulic diameter,  $\text{Pr}$  is the Prandtl Number and  $T_c$  with  $T_{\text{He}}$  are the temperatures of the conductor and the flowing helium, respectively. We also find that the Nusselt Numbers are large for our design of both LTS and HTS conductor lines suggesting that the convection will be a dominant process for the heat transfer.

Using the formula (3) we project ideal heat transfer for the proposed LTS and HTS conductors operating with supercritical helium of average 4.7 K temperature and 0.26 MPa pressure. We observe that the heat transfer increases by about a factor of 5 from 0.5 g/s to 5 g/s flow rate strongly indicating that higher flow rates in CICC conductors are beneficial for the heat transfer. But it is also interesting to note that the expected heat transfer saturates at flows of about 5 g/s to that of the LHe boiling off the metal surface.

The only available data [7] for the heat transfer in a CICC conductor suggests that the efficiency of the heat transfer is only at about 25%. In addition to that there is also a “delay in response” meaning that there is a time delay for the heat to be passed from the flowing liquid helium through the surface of the conductor to its interior. This time delay is very difficult to estimate as it depends strongly on the physical properties of both the contact surface and the conductor internal structure. The time delay, however, is very detrimental in a quench situation. For this reason superconductors should operate with wide temperature margins so the heat absorption can take place with as high efficiency as possible in the case of a quench.

As shown in figure 4, the effects of the helium flow rate on availability of the heat transfer, and on the pressure loss in the CICC conductors are contradicting each other. In an ideal case one would like to use the lowest possible liquid helium flow rate (but above the laminar state) to minimize the required power of the cryogenic plant. So, the efficiency of the heat transfer from the flowing liquid helium to the conductor strands is of greatest concern. Consequently, our CICC conductors were designed to optimize as much as possible the heat transfer. Both the HTS and the LTS conductors are designed with large void fractions (70%-80%), and with at least 50% of a direct contact area of strands to the helium coolant. In addition, the heat transfer through a convection process which is dominant one in our conductor line designs is viewed as the most efficient one.

## CRYOGENIC COOLING IN A MAGNET ENERGIZED BY A TRANSMISSION LINE CONDUCTOR

The arrangement of the conductor winding in a magnet plays a very significant role in the determination of the required cooling power per magnet length. In principle there are two options for the arrangement of conductor winding: (1) multiple turn, and (2) single turn. A multiple turn option is a standard one used in most accelerator magnet constructions. A single turn option is rather a novel approach for a large scale application and it was first proposed for the VLHC [8]. The two options of the conductor windings are shown in figure 5. In a single turn

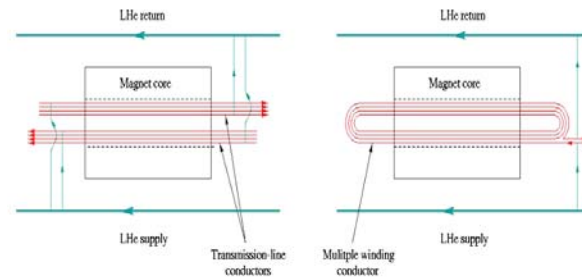


Fig. 5 Single and multiple winding magnet options

winding the liquid helium coolant can be supplied and returned in the path of the individual magnet length (or the selected magnet string). In a multiple turn winding the path of the liquid helium coolant is equal to that of the total length of the conductor winding. Consequently, the pressure drop of the liquid helium coolant in a magnet of  $N$ -turns conductor is at least  $N$  times larger than in a magnet of the same length but a single turn conductor. Naturally the drawback of a magnet with a single turn conductor is that the required current is  $N$  times higher. In the same time, however, the magnet inductance is  $N^2$  times lower. The low inductance of single turn conductor magnet minimizes the stored energy which helps for the quench protection but it increases the difficulty of the current regulation of a magnet string. The power supply design will need to manage both high current and small  $Ldi/dt$  voltage in fast-ramping and fast-cycling operations.

Accelerator magnet string of single turn conductors is powered by a transmission-line conductor with a single power supply. The liquid helium supply and return lines run parallel to the magnet string with inlets and exits for the individual magnets (or magnet string subsets) as required by the allowed pressure drop and temperature rise. Such arrangement is efficient for minimization of the required cryogenic power and it allows one to simplify magnet interconnections as illustrated in figure 6. The single turn HTS or LTS conductor lines can be easily bent in the horizontal plane to create space for the corrector magnets set. This is also a convenient area for splicing conductors and to provide inlet and outlet for liquid helium coolant.

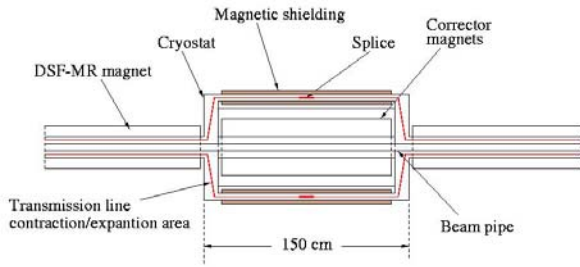


Fig.6 Top view of possible connection of 2 magnets in a transmission-line conductor arrangement with a step out around the corrector magnets

For the DSFMR accelerator the assumed length of a single magnet is 5 m which makes the single conductor length of minimum of 6 m. We use this conductor length to tentatively estimate the required cryogenic cooling power for the DSFMR accelerator based on the HTS and LTS conductor line designs described above. Assuming the initial liquid helium of 4.4 K and 2.6 bar we use the projections from figure 4 to calculate the pressure drop for a 5 m long magnet powered with 8 parallel conductor lines each of 6 m length, in a transmission-line mode of operations as indicated in figure 5. In order to project the ideal heat transfer we assume two values of the allowed temperature rise: (1) 0.03 K/m or 0.2 K/6m and (2) 0.1 K/m or 0.6 K/6m; with the first one assumed to be characteristic of the power loss in the HTS conductor [6] and the second one of the LTS one [5]. With 0.5 g/s flow rate we assume pressure drop to be 0.1 bar (figure 4) in both HTS and LTS lines. The initial helium coolant enthalpy is  $1.09284 \text{ e}^4 \text{ J/kg}$ , and the enthalpy after LHe flow through the 6 m long powered conductors is then  $1.19018 \text{ e}^4 \text{ J/kg}$  for the HTS case, and  $1.50288 \text{ e}^4 \text{ J/kg}$  for the LTS one. This leads to 0.49 W/6m and 2.05 W/6m of the used cryogenic power in the HTS and the LTS case, respectively. As there are 8 conductor lines per magnet the projected total used cooling power is about 3.9 W (HTS) and 16.4 W (LTS) for the magnets of 5 m length. This result produces the overall required DSFMR cryogenic power of  $\sim 8 \text{ kW}$  (HTS) and  $\sim 34 \text{ kW}$  (LTS). The 34 kW power projected with the LTS conductor much exceeds the currently available cryogenic power of 24 kW for the Tevatron operations.

### TEST ARRANGEMENT OF THE CONDUCTORS FOR THE FAST CYCLING MAGNET

The projections of the capability of cryogenic power for the fast cycling magnets powered with transmission line conductors presented above indicate that although there is a promising venue (especially with the HTS conductor) a strong R&D effort is required to actually measure this

capability as a function of both dynamic and static power losses before embarking on a serious accelerator design. With this in mind we have begun constructing a test setup for the fast cycling superconducting magnets at Fermilab. The test is located in E4R enclosure that is equipped with a cryoplant producing 5 g/s flow of supercritical helium (no power loss). The test arrangement is show in figure 7. The 1.3 m long test conductor lines will be placed inside the CDA magnet gap. The test conductor is connected to

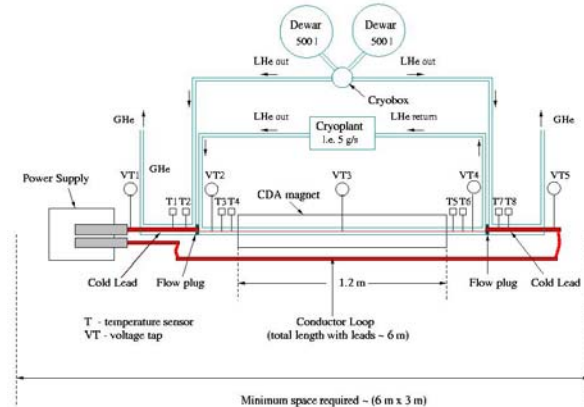


Fig. 7 Schematic view of the conductor test arrangement

the power supply through a water cooled copper conductor loop. The test conductor is connected to that loop through a pair of conventional leads. The test conductor is cooled with a supercritical helium flow while the leads are cooled independently with two-phase liquid helium supplied from 500 l dewars. The temperature at the inlet and outlet of the test conductor will be measured together with the helium flow rate from the cryoplant. The CDA magnet shown in figure 8 allows one to generate dipole fields of up to 0.7 T with repetition rate exceeding 50 Hz, if required. The dB/dt power loss will be measured with power supply off. The DSFMR magnet B-field is 2 T with a repetition rate of 0.5 Hz, so operating the



Fig. 8 CDA dipole for the HTS and LTS conductor tests CDA magnet at 0.7 T with repetition rates up to 5 Hz will exceed even multiple times the DSFMR magnet design parameters. The CDA magnet has a very large gap (82.5 mm height x 305 mm width) facilitating installation of the test conductors, and their removal from the magnet for e.g. the di/dt induced power loss measurements. For these measurements the power supply will be powered to

currents of up 10 kA. In spite of the large gap the B-field quality is rather good as indicated in figure 9 below.

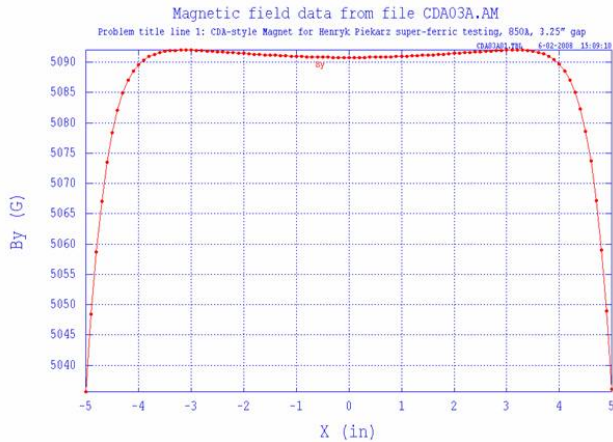


Fig. 9 CDA magnet B-field profile at 0.5 T

A schematic view of the HTS conductor assembly is shown in figure 1, and the connection of the conductor to the leads is shown in figure 10. This connection is arranged in a way that it will be possible to rotate the conductor relative to the dipole field lines in the CDA magnet gap. This will allow investigation of the HTS power losses as a function of the angle between the wide side of the tape and B-field orientation.

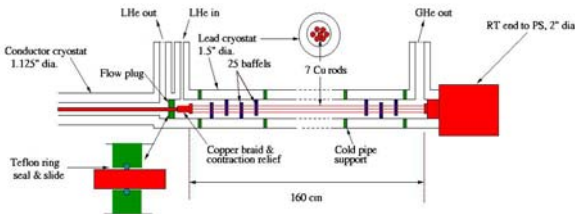


Fig. 10 A schematic view of current leads connection to the test conductor and the power supply

The engineering design in progress of the HTS conductor and the lead to conductor connection is shown in figures 11, 12. The engineering design of the LTS conductor, as conceptually shown in figure 1, will follow.

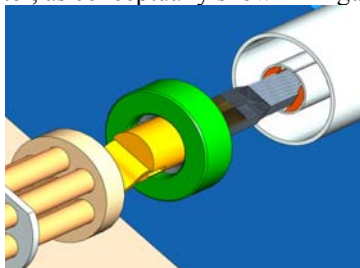


Fig. 11 A 3-D view of power lead end and its connection to superconductor line.

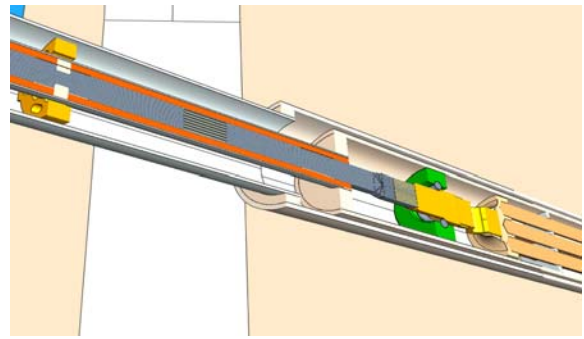


Fig.12 A horizontally sliced 3-D view of HTS conductor. Showing from left: cold pipe support (yellow), baffle (beige), HTS strands (grey), flow plug (green) and copper braid connection to copper rods of the lead (gold).

The power leads are scaled down from the VLHC-LF magnet design. Each lead is made of seven, 1/4" diameter, 160 cm length low resistance copper rods. The overall size of the lead assembly is designed to allow its passing through the CDA magnet gap facilitating change of the test conductors. The warm end of the lead is a 2" diameter copper rod that is only clamped to the power supply end thus allowing for the conductor assembly rotation inside the CDA magnet gap.

## REFERENCES

- [1] L. Bottura, "Fast cycled superconducting magnets for PS2", WAMSDO-08, CERN, May 19-23, 2008
- [2] H. Piekarz, S. Hays, Y. Huang and V. Shiltsev, Design Considerations of Fast-Cycling Synchrotrons Based on Superconducting Transmission Line Magnet", EPAC-2008, and FERMILAB-CONF-08-176 APC
- [3] G. Moritz, "Superconducting Magnets for the Intern. Accelerator Facility for Beams of Ions & Antiprotons at GSI", Applied Superconductivity Conf. Houston, TX August 4-9, 2002
- [4] H. Piekarz, S. Hays, Y. Huang, V. Kashikhin, G. de Rijk, L. Rossi, "Design Considerations for Fast-Cycling Superconducting Magnets of 2 T B-field Generated by a Transmission Line Conductor of up to 100 kA Current", MT-20, 2007
- [5] Meakawa, M.R. Smith, S.W. Sciver., "Pressure Drop Measurements of Prototype NET-CEA CICC Cond.", IEEE Trans. Apl. Superc., vol 5, no 2, 1995
- [6] Moody Diagram using the Darcy-Weibash equation, <http://en.wikipedia.org>
- [7] Y. Wachi, M. Ono, T. Hamajima, "Heat Transfer Characteristics of the Supercritical Helium in CICC Conductors", IEEE Trans. Apl. Superc. Vol 5, 1995
- [8] G. Ambrosio et al, "Design Study for a Staged Very Large Hadron Collider", Fermilab-TM-2149, 2001